Journal of Materials Chemistry A

Accepted Manuscript

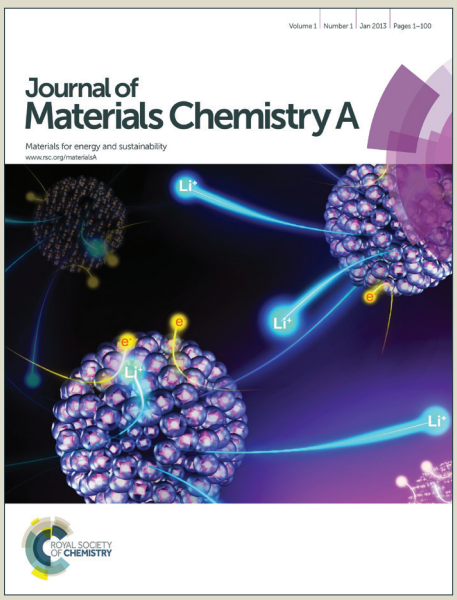

ROYAL SOCIETY OF CHEMISTRY

www.rsc.org/materialsA

Journal of

Materials Chemistry A

RSCPublishing

ARTICLE

One-step Synthesis of Zinc–cobalt Layered Double Hydroxide (Zn-Co-LDH) Nanosheets for High-efficiency Oxygen Evolution Reaction

Chen Qiao,[a] Yuan Zhang,[a,c] Youqi zhu,[b] Chuanbao Cao,[b] Xinhua Bao*[a] and Jiaqiang Xu*[a]

wasCite this: DOI: 10.1039/x0xx00000x

Received 00th January 2012,
Accepted 00th January 2012

DOI: 10.1039/x0xx00000x

www.rsc.org/

Two-dimensional (2D) nanomaterials show their great potential for electrocatalysis or other applications that require large surface area. In this work, we develop porous zinc-cobalt layered double hydroxide (Zn-Co-LDH) nanosheets by using one-step microwave-assisted approach, and examine their oxygen evolution reaction (OER) performance. The Zn-Co-LDH nanosheets with a high specific surface area of 116.4 m^2 g^{-1} exhibit good OER activity, expressed as low onset overpotential, small Tafel slope and large exchange current density. At the overpotential of 0.54 V, the current density of Zn-Co-LDH nanosheets is about 15.06 mA cm^{-2}, which is much higher than that of Zn-Co-LDH nanoparticles. The comparable electrocatalytic performance may be attributed to the porous 2D structure generating more active sites and higher electronic conductivity. Furthermore, the obtained Zn-Co-LDH nanosheets show good stability during long time running at 1.55 V vs. RHE. Accordingly, an effective OER catalyst is exploited by using a simple microwave-assisted synthesis. Such an effective method could be extended to large-scale synthesis of uniform and stable 2D LDH nanomaterials.

Introduction

Nowadays, the exhaustion of traditional energy and the deterioration of environment have been the serious consideration in current society.[1-4] Hence, the topics that find efficient electrocatalyst to solve energy problems are arousing the interest of many researchers. Oxygen evolution reaction (OER) is an important half reaction involved in many energy conversion and storage processes such as water splitting.[5, 6] Many researches have been focused on the design and controllable synthesis of OER catalysts. Noble metal catalysts like RuO_2 and IrO_2 exhibit high performance.[7, 8] Zhongbin Zhuang and co-workers[9] found that monodispere $Au@Co_3O_4$ core-shell exhibited excellent catalytic activity and great stability for OER in alkali solution. Tobias Reier and co-workers[10] reported that Ir nanoparticles showed good stability and high OER activity as nanoscaled OER catalyst. However, new catalysts with low cost, high activity and enhanced OER kinetics are continuously in great demand.[11-17]

Layered double hydroxides (LDHs) are a class of layered materials, in which the positively charged layers contains alternatively arranged metal cations (they are commonly divalent and trivalent, although monovalent metal cations are also known.[18, 19]) balanced by charge-compensating anions positioned within the interlayer space. Due to the rapid development of electrocatalysts, the study on the LDH for OER has attracted much attention.[20-22] Tewodros Asefa and co-workers[18] reported that the bimetallic Zn−Co layered double

[a]Department of Chemistry, Shanghai University, Shanghai 200444, China. E-mail: xujiaqiang@shu.edu.cn
[b]Research Center of Materials Science, Beijing Institute of Technology, Beijing 100081,China. E-mail: cbcao@bit.edu.cn; Fax: +86 10 68912001; Tel: +86 10 68913792.
[C] State Key Laboratory of Transducer Technology
Shanghai Institute of Microsystem and Information Technology
Chinese Academy of Sciences, Shanghai 200050 (China)

Electronic Supplementary Information (ESI) available: Turnover frequency (TOF) calculation and Electrochemical Measurements. See DOI: 10.1039/b000000x/

hydroxide (Zn−Co−LDH) can serve as an efficient electrocatalyst for water and alcohol oxidation, respectively.

Two-dimensional (2D) materials have larger active surface areas compared with other bulk counterparts.[23-28] Norskøv and his cooperators used density functional theory (DFT) to build a theoretical model for hydrogen evolution reaction (HER) based on the calculated adsorption energies.[29-31] In accordance with their results, the edge of lamellar MoS_2 revealed the reasonably high activity.[32] Hongjie Dai and his co-workers[33] found that NiFe-LDH nanoplates were highly active for oxygen evolution reaction in alkaline solutions. Fang Song and Xile Hu[34] showed that the higher OER activity of exfoliated LDHs was mainly attributed to an increase in the number of active edge sites and the higher electronic conductivity.

Liquid exfoliation of layered materials has emerged as a conventional method in producing novel two-dimensional materials.[35-37] However, because of the low yield and complex synthesis of two-dimensional materials from liquid exfoliation, it is expected to find simple and effective new ways to prepare 2D nanomaterials. In this work, one-step microwave-assisted approach was used for the preparation of Zn-Co-LDH nanosheets, which avoided the low yield and the complex synthesis via the liquid exfoliation method. Such a simple and effective method could be extended to a large-scale manufacture. The electrochemical measurement showed that Zn-Co-LDH nanosheets exhibited excellent catalytic activity and great stability for OER in alkali solution compared with Zn-Co-LDH nanoparticles. The improved electrocatalytic activity may be associated with 2D porous structure, generating favorable surface permeability and highly active surface area.

Materials synthesis

To synthesize Zn-Co-LDH nanosheets, 0.446 g of zinc nitrate hexahydrate (1.5 mmol), 0.873 g of cobalt nitrate hexahydrate (3 mmol) and 1.441 g of urea (24 mmol) were dissolved in 25 mL deionized water, and then 70 mL ethylene glycol was added in. The formed solution was transferred into a 350 mL homemade round-bottomed flask and treated under microwave irradiation in a XH-MC-1 microwave reactor at 900 W. After 20 min of microwave treatment, the reaction was cooled to room temperature naturally. The product was filtered, washed thoroughly with distilled water and absolute ethanol, and dried at 60 ℃ overnight.

Structure characterization

Powder X-ray diffraction measurements were performed with a Rigaku D-MAX/ IIA X-ray diffactometer in a scanning range of 5-70° (2θ) at a rate of 1.2° (2θ)/min with Cu Kα radiation. Scanning electron microscopy (SEM) (JMS-6700F) and transmission electron microscope (TEM) (JEM-2010F) was utilized for the investigation of the morphology and structure of the prepared materials. Surface groups were monitored by Fourier Transform Infrared Spectroscopy (FTIR) with an AVATRA370 FTIR instrument using KBr plates within 4500-500cm^{-1}.The N_2 adsorption-desorption analysis was carried out at liquid nitrogen temperature on an ASAP 2020 analyzer (Micromeritics Instruments, USA). The Brunauer-Emmett-Teller (BET) specific surface area was calculated using the BET equation. Desorption isotherm was used to determine the pore size distribution using the Barret-joyner-Halender (BJH) method. Atomic force microscopy (AFM) characterization was performed on Bruker instrument (MultiMode 8 system).

Electrochemical measurements

The catalytic performance of the LDH nanosheets for water oxidation was studied by using a three-electrode configuration connected to a potentiostat (CorrTest CS330). The counter electrode was platinum wire and the reference electrode was saturated calomel electrode (SCE). Linear sweep voltammetry (LSV) measurements were gained in an alkali solution (0.1 M KOH) at room temperature at the scan rate of 5 mV s^{-1}. For the purpose of comparison, the catalytic performance of materials was tested on a glass carbon working electrode under similar conditions. All potentials measurements were converted to the reversible hydrogen electrode (RHE) based on the following formula $E_{RHE} = E_{SCE} + 0.242 + 0.059$ pH (in volts). It should be noted that all of the current densities were normalized on the electrode areas and the measured potentials vs. SCE were converted to the Nernst equation ;the overpotential (η) was calculated according to the following formula: η(V)= E_{RHE} - 1.23V.[38]

Electrochemical impedance spectroscopy (EIS) measurements were performed at an applied potential of 0.6 V (vs. SCE) in 0.1 M KOH solution. The impedance spectra were recorded at room temperature in the frequency range of 100 kHz to 0.01 Hz. Prior to each measurement, the KOH solution was bubbled with high purity N_2.

Results and discussion

Here we develop a one-step microwave-assisted approach to synthesize nanosheets. The Zn-Co-LDH nanosheets synthesis at different microwave power and different reaction time were carried out. The results were shown in Fig. S1†. We found that the XRD peaks of Zn-Co-LDH nanosheets were getting stronger with the increase of microwave power, especially the peaks of (003), (006) and (113). Accordingly, we chose the microwave power of 900 W. In the control experiments at different microwave irradiation time, there was no obvious difference observed for the XRD patterns (Fig. S2†). We further carried out the morphology analysis over samples obtained at different microwave irradiation time. From the AFM images (Fig. S3†), we found that the reaction time had a

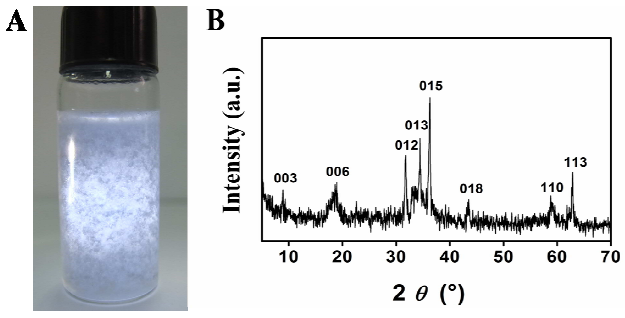

Fig.1 (A) Digital image (B) XRD pattern of Zn-Co-LDH nanosheets.

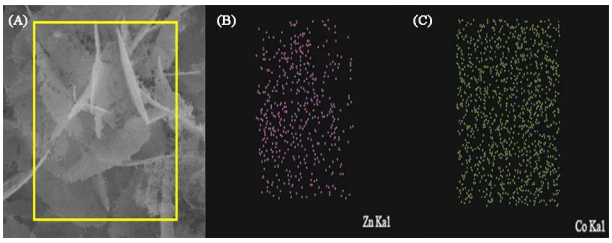

Fig. 2 (A) SEM image of Zn-Co-LDH nanosheets, (B) and (C) EDX mapping of Zn and Co elements

large effect on the morphology. The AFM images (Fig. S3†) clearly demonstrated that the size of Zn-Co-LDH nanosheets was getting larger with the increase of reaction time (from 5 min to 20 min). Further increasing the reaction from 20 min to 30 min, there was almost no obvious change on the morphology from the comparison of Fig. S3C† with Fig. S3D†. Therefore, the reaction time of 20 min and microwave power of 900W were chosen as the optimum conditions. Fig. 1A showed that the obtained product was chiffon-like suspended in water. XRD analysis result was shown in Fig. 1B. According to previous report, all of the diffraction peaks can be well indexed to a layered hydrotalcite-like phase.[18] The FTIR spectroscopy (shown in Fig. S4†) was carried out to determine the formation of double hydroxide. There were four obvious absorption bands in the region from 500 to 4000 cm^{-1}. The strong and broad IR absorption peak at ~3473 cm^{-1} was due to the stretching vibrations of OH groups. The relatively weak absorption at ~1580 cm^{-1} was attributed to the bending vibration of OH groups. The other two absorption bands at ~1348 and ~833 cm^{-1} were ascribed to the existence of CO_3^{2-}. These results indicated that there were a large number of OH groups, carbonates and water molecules existed in the Zn-Co-LDH material. Combined the XRD analysis result with FTIR spectroscopy, we can safely conclude that Zn−Co−LDH with the brucite-type layered structure was formed. A scanning electron microscopy (SEM) image of the as-synthesized Zn-Co-LDH nanosheets on conductive adhesive together with selected-area element analysis mapping of Zn and Co, showing that both Zn (purple) and Co (green) atoms were distributed through the whole area, revealing a homogeneous distribution of Zn and Co in the Zn−Co−LDH sample. The EDS analysis over the selected region from Table 1 showed that the atomic ratio between Zn and Co was approximate to 2:1, which was almost consistent with the initial metal precursor portions.

A typical SEM image (Fig. 3A) clearly demonstrated that a large number of uniform nanosheets were successfully prepared. The size of as-synthesized Zn-Co-LDH nanosheets was in the range of micrometer. The detailed morphology characterization was conducted by higher magnification SEM (shown in Fig. 3B). TEM observation (Fig. 3C) showed that the Zn-Co-LDH nanosheets were nearly transparent towards electron beam, which indicated the ultra-thin nature of the nanosheets. Further examination by higher magnification TEM confirmed that there were some small pores on the surface of nanosheets. Fig. 4 showed the peak-force-model atomic force microscopy (PF-AFM) images of the as-synthesized Zn-Co-LDH nanosheets on freshly cleaved mica. The PF-AFM observation indicated that Zn-Co-LDH nanosheets possessed a highly rough surface with defects and some small irregular pores. Both the height profile (see Fig. 4A) and the three-dimensional (3D) PF-AFM image (see Fig. 4B) indicated that the thickness of the as-prepared Zn-Co-LDH nanosheets about 2 nm. This special morphology may generate large specific surface area, and further providing high catalytic activity for OER. We also performed the BET analysis of obtained Zn-Co-LDH nanosheets. As been expected, the Zn-Co-LDH nanosheets exhibited porous structure and with a high specific

Table 1 The atomic ratio obtained from EDS analysis.

Element	Weight %	Atom%
C	43.42	62.55
O	26.85	29.04
Co	19.03	5.59
Zn	10.70	2.82
Total	100.00	100.00

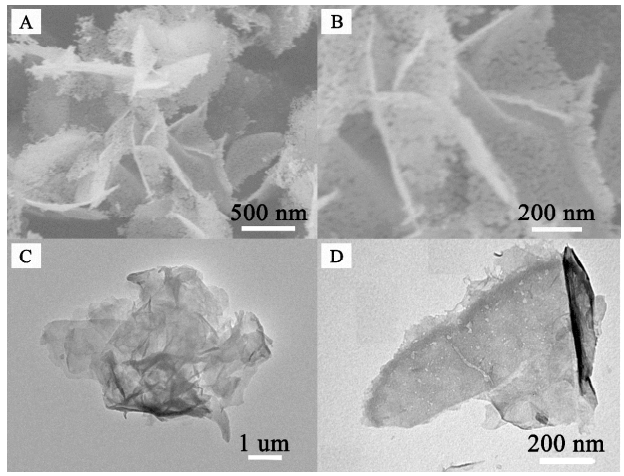

Fig. 3 (A) and (B) low- and high-magnification SEM images of the Zn-Co-LDH nanosheets. (C) and (D) TEM images of the Zn-Co-LDH nanosheets.

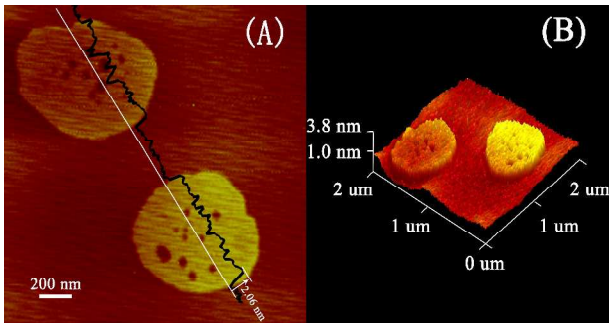

Fig. 4 A and B the height profile and the three-dimensional (3D) peak-force-model atomic force microscopy (PF-AFM) images of the as-synthesized Zn-Co-LDH nanosheets.

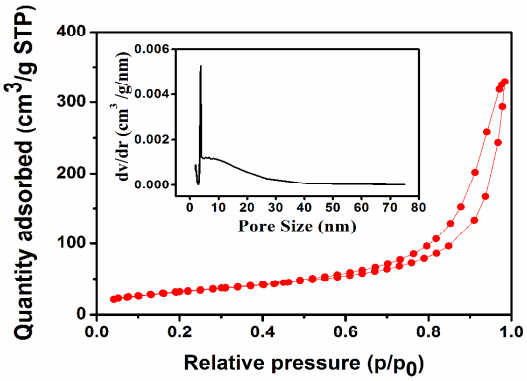

Fig. 5 Nitrogen adsorption isotherms and corresponding pore size distribution (inset) of the Zn-Co-LDH nanosheets.

surface area of 116.4 m^2 g^{-1} (Fig. 5). Such a characteristic structure could provide a large number of reactive sites and facilitate the transport of reactants and products effectively.

The electrocatalytic OER activities of Co-Zn-LDH were evaluated by a rotating disk electrode (RDE) in 0.1 M KOH solution. The rotating rate was kept at 2200 rpm to remove the generated oxygen bubbles. Firstly, we measured the polarization curves of Co-Zn-LDH sample. The OER activities of bulk $ZnCo_2O_4$, Zn-CO-LDH nanoparticles and Co_3O_4 nanopowders were included for comparison. From Fig. 6A, it can be seen that Zn-Co-LDH nanosheets catalyst showed the lowest onset potential and highest current density towards OER among these four catalysts, revealing the good OER activity. The detailed comparison on OER activities between Zn-Co-LDH nanosheets and other catalysts was performed. The comparison was made from onset potential, potential at a current density of 2 mA cm^{-2} and current density. The detailed results were shown in Table 2. Zn-Co-LDH nanosheets presented a lower overpotential (0.375 V) at the current density of 2 mA cm^{-2} than that of Zn-Co-LDH nanoparticles (0.46 V). At the overpotential of 0.54 V, the current density of Zn-Co-LDH nanosheets is about 15.06 mA cm^{-2}, which was much higher than that of other control samples. Fig . S5† showed the different current densities of different catalysts at a fixed overpotential of 0.375 V (0.6 V vs. SCE). The current density was about 1.98 mA cm^{-2} over Zn-Co-LDH nanosheets catalyst, which was about 5 times higher than that of other catalysts. Tewodros Asefa and co-workers[18] reported that the alternatively distributed bimetallic LDH structure provided a similar environment where the relatively inactive Zn^{2+} ions had a unique promoting effect, improving the interactions between reactants and active sites, further leaded to enhanced catalytic activity. It can be inferred that Zn itself may be not able to offer the catalytic function, while the alternative arrangement of Zn and Co in the LDH layer could be attributed to the improvement of catalytic performance.[22] We also investigated the OER activity of samples obtained at different reaction time. Form Fig. S9†, the OER activity of the sample obtained at 20 min was almost same as that of sample obtained at 30 min, which was much better than of the samples obtained at 5 min or 10 min. Here we found that the area of Zn-Co-LDH nanosheets had a powerful effect on OER activities (shown in Fig. S9†). The powerful effect can be explained by the edge of nanosheets owing reasonably high activity, which was consistent with previously reported results .[29-32]

To gain more insight into the OER activity, the comparison of Tafel plots with other catalysts was conducted, and the result was shown in Fig. 6B. Tafel plots were derived from the Tafel equation ($\eta = b \log j + \alpha$,where b is the Tafel slope).[36] From Fig. 6B, it could be seen that Co_3O_4 had a lower slop of 105 mV/decade, which was lower than that of Zn-Co-LDH

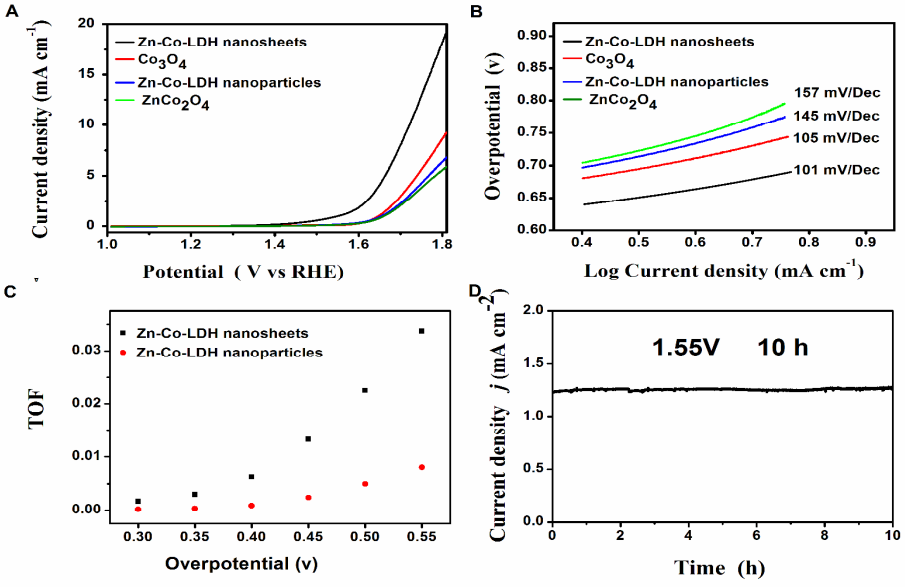

Fig. 6 (A) Linear sweep voltammograms of all catalytic electrodes in pH 13.0 KOH. The scanning rate was 5 mV s^{-1}. (B) Tafel plots of four catalysts loaded on GCE recorded in pH=13 KOH, corresponding to the LSV curves in Fig. 2A. (C) The derived TOF values of Zn-Co-LDH nanosheets and Zn-Co-LDH nanoparticles at different overpotentials in pH 13.0 KOH electrolyte, assuming all Co atoms are active sites.(D) A current–time curve obtained for water oxidation reaction in the presence of Zn–Co–LDH at 1.55 V vs. NHE.

Table 2 Electrochemical performance of Zn-Co-LDH nanosheets and the control samples.

Samples	η_{onset} (V)	$\eta_{2mA\ cm^{-2}}$ (V)	$I_{\eta=0.54\ V}$ (mA cm^{-2})
Zn-Co-LDH nanosheets	0.23	0.375	15.06
Zn-Co-LDH nanoparticles	0.35	0.461	5.15
Co_3O_4	0.32	0.447	6.80
$ZnCo_2O_4$	0.34	0.467	4.55
Zn-Co-LDH[a]	0.34	—	11.6
ZnCo-LDH-100[b]	0.33	0.427	13.3
Co-OH[c]	0.33	0.453	5.5
Zn-OH[c]	0.42	0.619	0.52

[a] Powder sample coated on a glassy carbon electrode reported in the literature. [18]

[b] nanowalls sample coated on a glassy carbon electrode reported in the literature. [22]

[c] Powder sample coated on a glassy carbon electrode reported in the literature. [22]

nanoparticles (145 mV/decade) and $ZnCo_2O_4$ (157mV/decade). It was well known that hydroxides had an intrinsically low conductivity than that of metal oxide. However, Zn-Co-LDH nanosheets had a slope of 101 mV/decade, which was much lower than that of Zn-Co-LDH nanoparticles. Especially, the slop of Zn-Co-LDH nanosheets was also lower than that of Co_3O_4. Therefore, Zn-Co-LDH nanosheets with porous ultra-thin two-dimensional structure exhibited better catalytic performance towards OER than that of Zn-Co-LDH nanoparticles and Co_3O_4. To further evaluate the catalytic performance of Zn-Co-LDH with different morphologies, their turnover frequencies (TOFs) at different overpotentials were calculated and plotted as a function of overpotential, assuming Faraday efficiency was 100% and every cobalt atom was an active site for OER.[39] As shown in Fig. 6C, the Zn-Co-LDH nanosheets and Zn-CO-LDH nanoparticles achieved 6.23×10^{-3} s^{-1} and 8.79×10^{-4} s^{-1} in KOH (pH=13.0) electrolyte solution at the overpotential of 0.4V. The Zn-Co-LDH nanosheets exhibited a 4.1 times higher current density than that of Zn-CO-LDH nanoparticles at overpotential of 0.55 V. This indicated that the higher activity was observed for the increase in the number of active edge sites and for higher electronic conductivity with nanosheets. Electrochemical impedance spectroscopy (EIS) was employed to study the interfacial properties of the modified electrodes. Generally, the depressed semicircle at high frequency was related to the electron transfer resistance at the electrode surface. The rapid electron transfer and faster OER kinetics on the surface of Zn−Co−LDH nanosheets electrode were confirmed by electrochemical impedance spectra (Fig. S10†), which showed a much lower Faradaic impedance for Zn−Co−LDH nanosheets than that of Zn-Co-LDH nanoparticles and Co_3O_4. Although the semicircle obtained from $ZnCo_2O_4$ was smaller than that of Zn-Co-LDH nanosheets, the faster OER kinetics and better OER activity on the surface of Zn-Co-LDH nanosheets electrode were confirmed by electrochemical performance measurements. The conductivity of materials may not be the only indicator for electro-catalytic properties. The good OER performance of Zn-Co-LDH nanosheets may be attributed to large enough interlayer spacing (with interlayer distance of about 0.9 nm) in this layered material. In this case, all the catalytically active Co species were assumed to exist on the reactive surface. The enough interlayer spacing would accelerate water molecules (reactants, whose diameter is about 0.32 nm) to diffuse into interlayers and reach to each Co sites, further facilitate OER activity.[40, 41]

The stability of Zn-Co-LDH nanosheets was also evaluated in a KOH aqueous solution (pH=13) at room temperature, the result was shown in Fig. 6D. The current density was almost retained during 10 h electrochemical running at 1.55 V (vs. RHE). Therefore, Zn-Co-LDH nanosheets could be promising OER catalyst with high activity and strong durability.

Conclusions

In summary, an effective microwave-assisted approach has been employed to synthesize Zn-Co-LDH nanosheets. This synthesis procedure was relatively simple, involving only metal precursors and urea. There was no need to consider the interferences from surfactants on electrocatalytic properties. Such a simple and effective method also could be extended to a large-scale manufacture. By comparing the electrocatalytic properties of Zn-Co-LDH nanosheets with Zn-Co-LDH nanoparticles, Zn-Co-LDH nanosheets showed more catalytic active sites and facilitated charge transfer of the composite electrodes. In addition, the obtained Zn-Co-LDH nanosheets exhibited higher activities and better stability towards OER. The results presented herein can be anticipated to give a fresh impetus to the rational design of other bi-materials LDH nanosheets with earth-abundant elements for catalysis and electrocatalysis applications.

Acknowledgements

We thank the help of AFM by Pengcheng Xu from State Key Laboratory of Transducer Technology Shanghai Institute of Microsystem and Information Technology Chinese Academy of Sciences.We also thank the supports of National Natural Science Foundation of China (No.61371021 and 51301101).

Notes and references

1. S. U. Khan, M. Al-Shahry and W. B. Ingler, Jr., *Science*, 2002, 297, 2243-2245.
2. J. R. McKone, N. S. Lewis and H. B. Gray, *Chemistry of Materials*, 2014, 26, 407-414.
3. Y. Zhang, T. Han, J. Fang, P. Xu, X. Li, J. Xu and C.-C. Liu, *Journal of Materials Chemistry A*, 2014, 2, 11400.
4. Y. Zhang, M. Janyasupab, C. W. Liu, X. X. Li, J. Q. Xu and C. C. Liu, *Advanced Functional Materials*, 2012, 22, 3570-3575.
5. F. Li, H. Gong, Y. Wang, H. Zhang, Y. Wang, S. Liu, S. Wang and C. Sun, *J. Mater. Chem. A*, 2014, 2, 20154-20163.
6. Y. V. Geletii, Z. Huang, Y. Hou, D. G. Musaev, T. Lian and C. L. Hill, *Journal of the American Chemical Society*, 2009, 131, 7522-7523.
7. H. G. Sanchez Casalongue, M. L. Ng, S. Kaya, D. Friebel, H. Ogasawara and A. Nilsson, *Angewandte Chemie*, 2014, 53, 7169-7172.
8. T. Reier, M. Oezaslan and P. Strasser, *Acs Catalysis*, 2012, 2, 1765-1772.
9. Z. Zhuang, W. Sheng and Y. Yan, *Advanced materials*, 2014, 26, 3950-3955.
10. T. Reier, I. Weidinger, P. Hildebrandt, R. Kraehnert and P. Strasser, *Ecs Transactions*, 2013, 58, 39-51.

11. M. García-Mota, M. Bajdich, V. Viswanathan, A. Vojvodic, A. T. Bell and J. K. Nørskov, *The Journal of Physical Chemistry C*, 2012, 116, 21077-21082.
12. X. Zhou, Z. Xia, Z. Zhang, Y. Ma and Y. Qu, *Journal of Materials Chemistry A*, 2014, 2, 11799.
13. L. Trotochaud, J. K. Ranney, K. N. Williams and S. W. Boettcher, *Journal of the American Chemical Society*, 2012, 134, 17253-17261.
14. S. Chen, J. J. Duan, J. R. Ran, M. Jaroniec and S. Z. Qiao, *Energy & Environmental Science*, 2013, 6, 3693-3699.
15. D. Wang, X. Chen, D. G. Evans and W. Yang, *Nanoscale*, 2013, 5, 5312-5315.
16. T. Y. Ma, S. Dai, M. Jaroniec and S. Z. Qiao, *Angewandte Chemie*, 2014, 53, 7281-7285.
17. S. Mao, Z. Wen, T. Huang, Y. Hou and J. Chen, *Energy & Environmental Science*, 2014, 7, 609.
18. X. Zou, A. Goswami and T. Asefa, *Journal of the American Chemical Society*, 2013, 135, 17242-17245.
19. C. Gomes Silva, Y. Bouizi, V. Fornes and H. Garcia, *Journal of the American Chemical Society*, 2009, 131, 13833-13839.
20. J. S. Kanady, E. Y. Tsui, M. W. Day and T. Agapie, *Science*, 2011, 333, 733-736.
21. Z. Lu, W. Xu, W. Zhu, Q. Yang, X. Lei, J. Liu, Y. Li, X. Sun and X. Duan, *Chemical communications*, 2014, 50, 6479-6482.
22. Y. Li, L. Zhang, X. Xiang, D. P. Yan and F. Li, *Journal Of Materials Chemistry A*, 2014, 2, 13250-13258.
23. Y. Zhu, C. Cao, S. Tao, W. Chu, Z. Wu and Y. Li, *Sci Rep*, 2014, 4, 5787.
24. D. Voiry, H. Yamaguchi, J. Li, R. Silva, D. C. Alves, T. Fujita, M. Chen, T. Asefa, V. B. Shenoy, G. Eda and M. Chhowalla, *Nature materials*, 2013, 12, 850-855.
25. X. Ge, C. D. Gu, X. L. Wang and J. P. Tu, *Journal Of Materials Chemistry A*, 2014, 2, 17066-17076.
26. S. Y. Tai, C. J. Liu, S. W. Chou, F. S. S. Chien, J. Y. Lin and T. W. Lin, *Journal Of Materials Chemistry*, 2012, 22, 24753-24759.
27. Y. Q. Zhu, H. Z. Guo, Y. Wu, C. B. Cao, S. Tao and Z. Y. Wu, *Journal Of Materials Chemistry A*, 2014, 2, 7904-7911.
28. D. H. Nagaraju, Q. Wang, P. Beaujuge and H. N. Alshareef, *J. Mater. Chem. A*, 2014, 2, 17146-17152.
29. M. Chhowalla, H. S. Shin, G. Eda, L. J. Li, K. P. Loh and H. Zhang, *Nature chemistry*, 2013, 5, 263-275.
30. J. K. Norskov, T. Bligaard, J. Rossmeisl and C. H. Christensen, *Nature chemistry*, 2009, 1, 37-46.
31. J. K. Nørskov, T. Bligaard, A. Logadottir, J. R. Kitchin, J. G. Chen, S. Pandelov and U. Stimming, *Journal of The Electrochemical Society*, 2005, 152, J23.
32. J. Bonde, P. G. Moses, T. F. Jaramillo, J. K. Nørskov and I. Chorkendorff, *Faraday Discussions*, 2009, 140, 219.
33. M. Gong, Y. Li, H. Wang, Y. Liang, J. Z. Wu, J. Zhou, J. Wang, T. Regier, F. Wei and H. Dai, *Journal of the American Chemical Society*, 2013, 135, 8452-8455.
34. F. Song and X. Hu, *Nature communications*, 2014, 5, 4477.
35. V. Nicolosi, M. Chhowalla, M. G. Kanatzidis, M. S. Strano and J. N. Coleman, *Science*, 2013, 340, 1420-+.
36. S. Chen and S. Z. Qiao, *ACS nano*, 2013, 7, 10190-10196.
37. J. B. Han, X. Y. Xu, X. Y. Rao, M. Wei, D. G. Evans and X. Duan, *Journal Of Materials Chemistry*, 2011, 21, 2126-2130.
38. M. W. Kanan and D. G. Nocera, *Science*, 2008, 321, 1072-1075.
39. Y. Surendranath, M. W. Kanan and D. G. Nocera, *Journal of the American Chemical Society*, 2010, 132, 16501-16509.
40. G. R. Williams and D. O'Hare, *Journal Of Materials Chemistry*, 2006, 16, 3065-3074.
41. A. I. Khan and D. O'Hare, *Journal Of Materials Chemistry*, 2002, 12, 3191-3198.